

Shape transition in very large germanium islands on Si(111)

J. M. MacLeod,^{1,a)} J. A. Lipton-Duffin,^{1,b)} U. Lanke,² S. G. Urquhart,² and F. Rosei^{1,c)}

¹INRS-EMT, Université du Québec, 1650 Boulevard Lionel-Boulet, Varennes, QC J3X 1S2, Canada

²Department of Chemistry, University of Saskatchewan, Saskatoon, SK S7N 5C9, Canada

(Received 5 December 2008; accepted 11 February 2009; published online 11 March 2009)

Ge islands with areas up to hundreds of μm^2 were grown on Si(111). These islands, grown above 750 °C and at a deposition rate of 1 monolayer/min, become decreasingly compact with increasing size and can have nonuniform cross sections with heights reaching over 500 nm. The largest islands are ramified, often comprising multiple discrete parts. X-ray photoemission electron microscopy absorption maps show that the islands have a higher concentration of Ge at their centers, with more Si near the edges. We propose that the shape transformation is driven by strain relief at the island perimeters. © 2009 American Institute of Physics. [DOI: 10.1063/1.3093674]

The growth of Ge films on Si has been the subject of intense study for two decades.^{1–4} The defining characteristic of Ge/Si growth is the formation of three-dimensional islands that occur after the completion of an initial pseudomorphic wetting layer (WL). Due to Si–Ge alloying,^{5–10} the *effective* lattice mismatch is much smaller than the actual 4.2% misfit between Ge and Si, so the growth is often referred to as *modified* Stranski–Krastanov. On Si(001) this strain also has an important effect on the shape of the islands, which undergo an abrupt transition from pyramidal to dome shape with increasing island size.^{11–13} On Si(111), no such transitions have been identified.

Using high growth temperatures and relatively low deposition rates, we succeeded in routinely growing islands with lateral dimensions over tens of μm^2 . With increasing size, the islands became decreasingly compact. The largest structures observed are “archipelagos” of ramified islands. The growth of two-dimensional ramified islands has been reported for metal-on-metal heteroepitaxy, both on triangular^{14–17} and square substrate lattices,¹⁸ and recently for submonolayer Si homoepitaxy.¹⁹ It has also been reported for Pb-mediated submonolayer growth of Ge on Si(111).²⁰ In this letter, we report the growth of large ramified Ge islands on Si(111).

P-type (111)-oriented Si wafers, B-doped to ≈ 15 , were flash cleaned by electron bombardment. During Ge deposi-

tion, samples were held at temperatures of 770, 780, and 785 °C (± 15 °C), measured using an infrared pyrometer. Ge was deposited from an electron beam evaporator at a nominal rate of ≈ 1 monolayer (ML)/min to a nominal thickness of ≈ 30 ML. Each sample was held at the growth temperature for 5 min following Ge deposition. X-ray photoemission electron microscopy (XPEEM) measurements were performed on freshly prepared samples at the spectromicroscopy (SM) beamline of the Canadian Light Source (CLS) synchrotron using an Elmitec PEEM III with an energy filter.²¹ All other characterizations were carried out *ex situ*. Atomic force microscopy (AFM) measurements were performed under ambient conditions with a Digital Instruments EnviroScope in tapping mode. AFM images were processed using the WSM software.²² Measurement of island areas and perimeters was done with the IMAGE SXM software.²³

Figure 1 is a panel of five AFM images, each showing an island and a portion of the surrounding WL. The figure shows the prototypical island shapes observed: [Fig. 1(a)] irregular hexagons, [Fig. 1(b)] triangles, [Fig. 1(c)] trilliums, and ramified islands, which are most often observed [Fig. 1(d)] in trios and in [Fig. 1(e)] archipelagos of roughly triangular shape.²⁴ The substrate around each island has been etched away to a depth of ≈ 100 nm. The hexagonal and triangular islands [Figs. 1(a) and 1(b)] have divots at their centers, but are otherwise quite uniform in height over their

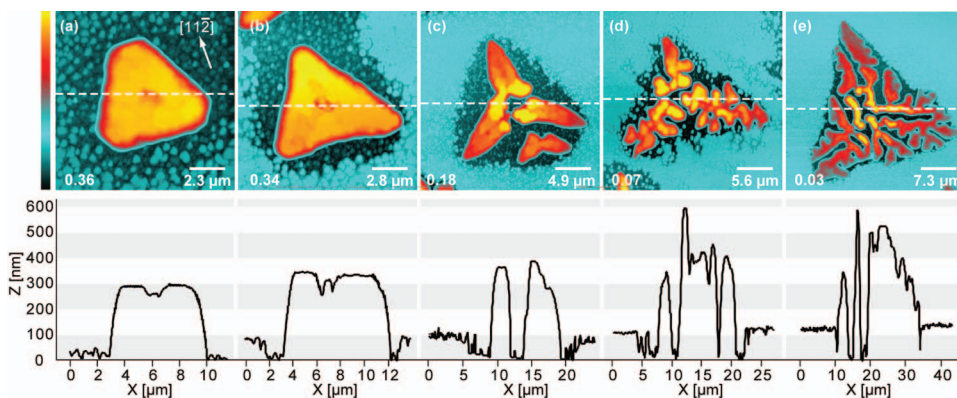


FIG. 1. (Color) AFM images and sections illustrating the morphologies of Ge islands. Prototypical islands with (a) hexagonal, (b) triangular, and (c) trillium shapes are shown, as well as ramified islands with (d) threefold and (e) triangular profiles. The number in the lower left corner of each image is the circularity ratio (see text) of the island or collection of islands. All islands were present on the same sample; the crystallographic direction specified in (a) applies to all images.

a)Electronic mail: macleod@emt.inrs.ca.

b)Present address: Dipartimento di Fisica, Università degli Studi di Trieste, Trieste (TS), 34127, Italy.

c)Electronic mail: rosei@emt.inrs.ca.

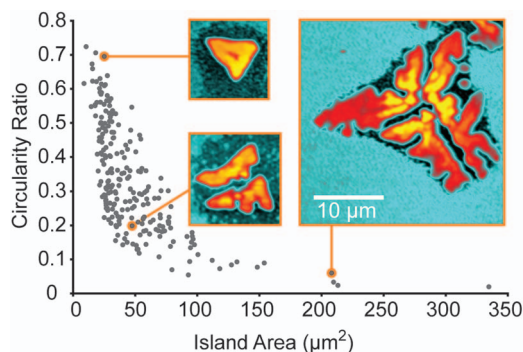


FIG. 2. (Color) Circularity ratio as a function of island area. The inset images show AFM topographs of the islands corresponding to individual data points. The images are presented at an identical scale, indicated by the scale bar in the largest image.

area. Conversely, the archipelagos [Figs. 1(d) and 1(e)] have very irregular height profiles, particularly near their centers, where the islands can be etched into the underlying substrate and can also rise to heights over 500 nm.

By evaluating samples grown at 770, 780, and 785 °C, we were able to correlate an increase in the density of large islands with an increase in substrate temperature.²⁵ The prototype islands shown in Fig. 1 represent discrete points on a continuum of island shapes. Triangular islands with indentations on their long sides, intermediate between triangular and trillium shapes, were often observed and islands larger than that shown in Fig. 1(e), but with the same qualitative appearance, were also identified. To investigate the relationship between the islands' shapes and sizes, AFM topographs of over 250 islands were analyzed. Figure 2 shows the circularity ratio, defined as $C=4\pi(\text{area})/(\text{perimeter})^2$, as a function of island area. The trend of the plot demonstrates that island compactness decreases with area.

Synchrotron XPEEM was used in x-ray absorption spectroscopy mode to create surface composition maps, obtained by integrating a series of images acquired above the transition edge and normalizing to an image taken below it. Figure 3 shows four elemental maps taken using this technique: Figs. 3(c) and 3(d) correspond to the Ge $2p_{3/2}$ edge (1217 eV) and Figs. 3(e) and 3(f) correspond to the Si $1s$ edge (1839 eV). The Ge-sensitive images [Figs. 3(c) and 3(d)] clearly show that the highest concentrations of Ge are found near island centers. Conversely, Figs. 3(b) and 3(d) show that the highest Si concentrations are found in the substrate region between the islands. These results qualitatively agree with previous x-ray photoemission spectroscopy (XPS) XPEEM maps of smaller Ge islands on Si(111).²⁶ Comparison with the topographic information²⁷ in images Figs. 3(a) and 3(b) reveals that etched regions around the islands are less rich in Si than regions where the WL is not noticeably disturbed by the presence of the islands.

The morphological and compositional analyses provide evidence for the incorporation of Si in the islands. The deeply etched regions around the islands, apparent in AFM images, are an obvious source for this Si. These regions do not exhibit an accretion of material at their outer edges, implying that the material must be incorporated into the islands.²⁸ The XPEEM data corroborate the morphological evidence for Si incorporation: the inhomogeneous concentration of Ge on the island surface implies that Si is present in

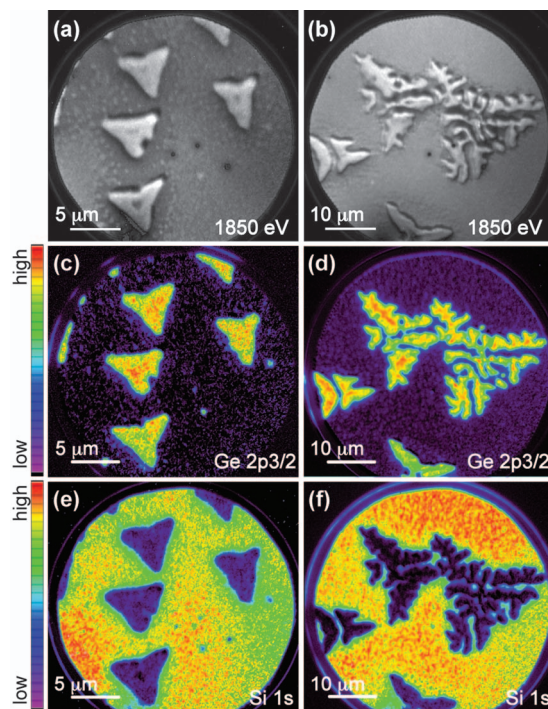


FIG. 3. (Color) XPEEM images [(a) and (b)] and absorption spectroscopy maps of the [(c) and (d)] Ge and [(e) and (f)] Si distributions in typical islands. The color scale in (c)–(f) has been scaled to each image individually in order to highlight the variation in concentration.

non-negligible amounts, particularly around the perimeters of the islands.

Despite a relatively low effective lattice mismatch due to Si alloying, hallmarks of strain relief dominate the structure of the observed islands. The etched regions around the islands result from the motion of atoms away from highly strained regions.²⁹ Similarly, the depleted regions at island centers are consistent with the removal of material from a region of relatively high strain, the Ge-rich island centers. The largest islands exhibit deep etched chasms at their centers. The extra material accumulated around these etched regions implies that the removed material is redistributed back into the island itself and is not removed to the epilayer. This accretion corresponds to regions where the largest islands' heights typically exceed 500 nm.³⁰

The strain-driven shape transition on Si(001) (Ref. 11) and theoretical predictions that elastic relaxation can occur through a shape transition to less compact forms as strained islands grow in size³¹ indicate that the islands' shape transition is likely strain driven. The maximization of the perimeter then provides a mechanism for strain relief. A similar shape transition in a two-dimensional metal-on-metal system was attributed to the outward relaxation of undercoordinated atoms at the periphery of the strained islands.¹⁸ The same mechanism may be at work here, although dislocations at the island perimeter³² could also be a driving force for perimeter maximization. We note that in further analogy to Ge on Si(001),³³ surface diffusion may also play a key role in this shape transformation, and that anisotropic corner³⁴ or edge³⁵ diffusion, or an anisotropy in growth velocity,² could all have important consequences for the island shape.

We demonstrated the growth of very large Ge islands at the Si(111) surface. By employing relatively high growth temperatures (over 750 °C) and relatively low Ge

flux (1 ML/min), islands were grown to lateral dimensions of tens of microns with some cross-sectional features of over 500 nm in height. The shape of the islands varied with size, from compact triangular islands at smaller sizes to very large archipelagos of ramified islands. XPEEM data show that the island surface composition is inhomogeneous, with Ge concentrated at the center. We observed a continuous transition from compact to noncompact island shapes with size, yet we do not interpret this unequivocal evidence against an abrupt transition. More detailed studies of large triangular islands may reveal a critical size at which the transition toward ramification begins. Future experiments using low energy electron microscopy will address the growth mechanism of the island archipelagos and whether lateral island motion³⁶ is involved in this process. Additional XPEEM experiments will allow the creation of quantitative chemical maps of the islands.^{26,37}

This research was supported by the NSERC of Canada and the Canada Foundation for Innovation. F.R. is grateful to the Canada Research Chairs program for salary support. We also thank G. P. Lopinski for the use of his pyrometer and P. Raiteri for a helpful discussion of this work.

- ¹K. Brunner, *Rep. Prog. Phys.* **65**, 27 (2002).
- ²B. Voigtlander, *Surf. Sci. Rep.* **43**, 127 (2001).
- ³N. Motta, *J. Phys.: Condens. Matter* **14**, 8353 (2002).
- ⁴F. Rosei, *J. Phys.: Condens. Matter* **16**, S1373 (2004).
- ⁵M. De Seta, G. Capellini, F. Evangelisti, and C. Spinella, *J. Appl. Phys.* **92**, 614 (2002).
- ⁶F. Boscherini, G. Capellini, L. Di Gaspare, F. Rosei, N. Motta, and S. Mobilio, *Appl. Phys. Lett.* **76**, 682 (2000).
- ⁷F. Boscherini, G. Capellini, L. Di Gaspare, M. De Seta, F. Rosei, A. Sgarlata, N. Motta, and S. Mobilio, *Thin Solid Films* **380**, 173 (2000).
- ⁸F. Rosei, N. Motta, A. Sgarlata, G. Capellini, and F. Boscherini, *Thin Solid Films* **369**, 29 (2000).
- ⁹N. Motta, F. Rosei, A. Sgarlata, G. Capellini, S. Mobilio, and F. Boscherini, *Mater. Sci. Eng., B* **88**, 264 (2002).
- ¹⁰F. Rosei and P. Raiteri, *Appl. Surf. Sci.* **195**, 16 (2002).
- ¹¹G. Medeiros-Ribeiro, A. M. Bratkovski, T. I. Kamins, D. A. A. Ohlberg, and R. S. Williams, *Science* **279**, 353 (1998).
- ¹²F. M. Ross, J. Tersoff, and R. M. Tromp, *Phys. Rev. Lett.* **80**, 984 (1998).
- ¹³J. A. Floro, E. Chason, S. R. Lee, R. D. Twisten, R. Q. Hwang, and L. B. Freund, *J. Electron. Mater.* **26**, 969 (1997).
- ¹⁴H. Röder, K. Bromann, H. Brune, and K. Kern, *Phys. Rev. Lett.* **74**, 3217 (1995).
- ¹⁵R. Q. Hwang, J. Schröder, C. Günther, and R. J. Behm, *Phys. Rev. Lett.* **67**, 3279 (1991).
- ¹⁶T. Michely, M. Hohage, M. Bott, and G. Comsa, *Phys. Rev. Lett.* **70**, 3943 (1993).
- ¹⁷H. Brune, H. Röder, K. Bromann, K. Kern, J. Jacobsen, P. Stoltze, K. Jacobsen, and J. Nørskov, *Surf. Sci.* **349**, L115 (1996).
- ¹⁸B. Müller, L. Nedelmann, B. Fischer, H. Brune, J. V. Barth, and K. Kern, *Phys. Rev. Lett.* **80**, 2642 (1998).
- ¹⁹R. Dana and Y. Manassen, *Europhys. Lett.* **79**, 16001 (2007).
- ²⁰T. C. Chang, I. S. Hwang, and T. T. Tsong, *Phys. Rev. Lett.* **83**, 1191 (1999).
- ²¹U. D. Lanke, A. P. Hitchcock, P. Hitchcock, J. S. Ornstein, K. Kaznatcheev, A. Kolmakov, I. Annesley, A. McCready, and S. G. Urquhart, *IPAP Conf. Ser.* **7**, 85 (2006).
- ²²I. Horcas, R. Fernandez, J. M. Gomez-Rodriguez, J. Colchero, J. Gomez-Herrero, and A. M. Baro, *Rev. Sci. Instrum.* **78**, 013705 (2007).
- ²³S. D. Barrett, IMAGE SXM, <http://www.ImageSXM.org.uk>, 2008.
- ²⁴The islands exhibit the threefold symmetry of the Si substrate and have apexes extending along $\{11\bar{2}\}$. The individual branches of the ramified islands similarly align roughly along these directions.
- ²⁵The temperature dependence of the island shape was not rigorously determined in this study, since the size and shape of the islands on each sample varied over each sample due to heating inhomogeneities introduced by the sample holder.
- ²⁶F. Ratto, A. Locatelli, S. Fontana, S. Kharrazi, S. Ashtaputre, S. K. Kulkarni, S. Heun, and F. Rosei, *Small* **2**, 401 (2006).
- ²⁷Although XPEEM images are not strictly topographic, in our view, these images are indicative of topography due to the high x-ray energy and based on comparison with AFM images of the same samples.
- ²⁸X. Z. Liao, J. Zou, D. J. H. Cockayne, Z. M. Jiang, X. Wang, and R. Leon, *Appl. Phys. Lett.* **77**, 1304 (2000).
- ²⁹S. A. Chaparro, Y. Zhang, and J. Drucker, *Appl. Phys. Lett.* **76**, 3534 (2000).
- ³⁰These islands are considerably taller than the flat, compact islands observed at lower growth temperatures, such as the 8 nm tall, 70 nm wide islands grown at 350 °C (Ref. 2).
- ³¹J. Tersoff and R. M. Tromp, *Phys. Rev. Lett.* **70**, 2782 (1993).
- ³²F. K. LeGoues, M. Horn-Von Hoegen, M. Copel, and R. M. Tromp, *Phys. Rev. B* **44**, 12894 (1991).
- ³³F. Montalenti, P. Raiteri, D. B. Migas, H. von Känel, A. Rastelli, C. Manzano, G. Costantini, U. Denker, O. G. Schmidt, K. Kern, and L. Miglio, *Phys. Rev. Lett.* **93**, 216102 (2004).
- ³⁴H. Brune, H. Roder, K. Bromann, K. Kern, J. Jacobsen, P. Stoltze, K. Jacobsen, and J. Nørskov, *Surf. Sci.* **349**, L115 (1996).
- ³⁵H. Brune, H. Roder, K. Bromann, and K. Kern, *Thin Solid Films* **264**, 230 (1995).
- ³⁶U. Denker, A. Rastelli, M. Stoffel, J. Tersoff, G. Katsaros, G. Costantini, K. Kern, N. Y. Jin-Phillipp, D. E. Jesson, and O. G. Schmidt, *Phys. Rev. Lett.* **94**, 216103 (2005).
- ³⁷We were unable to carry out full quantitative XPS mapping due to the relatively large focused spot size ($\sim 30 \mu\text{m}$) at the SM beamline of the CLS.